Evidence for a Global Seismic-Moment Release Sequence

by Charles G. Bufe and David M. Perkins

Abstract   Temporal clustering of the larger earthquakes (foreshock-mainshock-aftershock) followed by relative quiescence (stress shadow) are characteristic of seismic cycles along plate boundaries. A global seismic-moment release history, based on a little more than 100 years of instrumental earthquake data in an extended version of the catalog of Pacheco and Sykes (1992), illustrates similar behavior for Earth as a whole. Although the largest earthquakes have occurred in the circum-Pacific region, an analysis of moment release in the hemisphere antipodal to the Pacific plate shows a very similar pattern. Monte Carlo simulations confirm that the global temporal clustering of great shallow earthquakes during 1952–1964 at $\mathbf{M} \geq 9.0$ is highly significant (4% random probability) as is the clustering of the events of $\mathbf{M} \geq 8.6$ (0.2% random probability) during 1950–1965. We have extended the Pacheco and Sykes (1992) catalog from 1989 through 2001 using Harvard moment centroid data. Immediately after the 1950–1965 cluster, significant quiescence at and above $\mathbf{M}$ 8.4 begins and continues until 2001 (0.5% random probability). In alternative catalogs derived by correcting for possible random errors in magnitude estimates in the extended Pacheco–Sykes catalog, the clustering of $\mathbf{M} \geq 9$ persists at a significant level. These observations indicate that, for great earthquakes, Earth behaves as a coherent seismotectonic system. A very-large-scale mechanism for global earthquake triggering and/or stress transfer is implied. There are several candidates, but so far only viscoelastic relaxation has been modeled on a global scale.

Introduction

Over the years global seismicity and energy and moment release patterns have been studied by investigators including Benioff (1951, 1954), Davies and Brune (1971), Mogi (1974, 1979), Kagan and Jackson (1991), Pacheco and Sykes (1992), Romanowicz (1993), Bufe (1997), and many others. The ongoing computation of seismic moment for worldwide earthquakes since 1977 by Dziewonski and others at Harvard (e.g., Dziewonski, *et al.*, 2001) and the compilation of a homogeneous moment catalog for large shallow earthquakes (1900–1989) by Pacheco and Sykes (1992) at Lamont have provided high-quality data sets that were lacking in the early studies. In this study we focus on the larger events of $\mathbf{M} \geq 8.2$ that dominate the cumulative moment history. We first examine the statistical significance of the observed clustering of the largest earthquakes in the catalog and of the extended period of low-moment release that follows. We then examine in detail the 1925–2001 window of order, a statistically significant and interesting pattern of moment release that occupies the most reliable 75% of the catalog and resembles one complete seismic cycle and possibly the beginning of another.

Earthquake Catalog

The pattern of global seismic-moment release described here is based on the Pacheco–Sykes moment catalog of large ($\mathbf{M} \geq 7$), shallow ($z < 70$ km) earthquakes. Pacheco and Sykes (1992), in deriving magnitude corrections to produce a homogeneous (1900–1989) catalog, relied on the assumption that the worldwide rate of occurrence of smaller ($\mathbf{M}$ 7) earthquakes does not change systematically over time. Nevertheless, they caution that the moment uncertainties during the first-quarter century are large. In this article we deal primarily with post-1925 data, extended through 2001 with data from the Harvard Centroid Moment Tensor catalog (for example, Dziewonski *et al.*, 2001). We used the Harvard data to ensure homogeneity with the 1900–1989 Pacheco–Sykes catalog.

In the interest of compact notation, the moments may be expressed in terms of moment magnitudes ($\mathbf{M}$) in the text. Moment magnitudes (Hanks and Kanamori, 1979) of events cited in this article are derived from the catalog scalar moments in Newton meters using

$$\mathbf{M} = (\log M_0 - 9.05) / 1.5. \qquad (1)$$

The practice has been to round the computed moment magnitude to two significant figures, such that $8.95 \leq \mathbf{M} < 9.05$ would be rounded to 9.0. The preferred (first listed) moments in the Pacheco–Sykes catalog were used for all events except the 1960 Chile earthquake, where a lower value of $2000 \cdot 10^{20}$ N m, $\mathbf{M}$ 9.5 (Kanamori and Anderson, 1975a) was used. Moments for this great event that are based on geodetic observations are even smaller (Plafker and Savage, 1970; Barrientos and Ward, 1991). Seismological moment determinations, such as the $2700 \cdot 10^{20}$ N m ($\mathbf{M}$ 9.6) estimate of Kanamori and Cipar (1974), tend to run higher. The Pacheco–Sykes preferred moment of $3200 \cdot 10^{20}$ N m, $\mathbf{M}$ 9.6 (Cifuentes and Silver, 1989) is based on a reanalysis of free oscillations first examined by Kanamori and Anderson (1975b), who had estimated a moment of $2000 \cdot 10^{20}$ N m for the mainshock and found evidence of an equally large, precursory slow event. Both studies determine total moment release (mainshock plus precursor) in excess of $4000 \cdot 10^{20}$ N m, equivalent to $\mathbf{M}$ 9.7, over a period of about 15 min. An $\mathbf{M}$ 8.2 foreshock (calculated as previously) had occurred the day before about 150 km to the north and ruptured toward the epicenter of the great 1960 Chile event, which in turn ruptured almost unilaterally to the south (Cifuentes, 1989) for a total rupture length in excess of 1000 km. Although the scalar moment of the great 1960 earthquake may be uncertain, it is clear that this earthquake is the largest in the twentieth century. If there is a global mainshock, this event is the prime candidate.

The largest earthquakes in the catalog dominate cumulative seismic-moment release. The great earthquakes that are observed as most influencing the rate of moment release, directly or indirectly, are of $\mathbf{M}$ 8.2 or larger. Events in this magnitude range are shown in Table 1. The great earthquakes cited in this article are identified by number in Figure 1.

Clustering and Quiescence

Principal clusters and gaps in the temporal distribution of great earthquakes with moment magnitudes calculated as previously are identified in Figure 2. They are modeled by a Monte Carlo simulation technique to determine probabilities of random occurrence. For each cluster or gap, 100,000 sequences of 100 years each were simulated to determine the probability of obtaining the observed clusters and gaps by chance. The results are shown in Figure 3. The greatest of the great earthquakes, those of $\mathbf{M} \geq 9.0$, cluster in a period of 11.4 yr during 1952–1964. For three random events during a 100-yr period, there is a 4% chance of such clustering. Seven of nine earthquakes of $\mathbf{M} \geq 8.6$ cluster within a period of 14.5 yr between 1950 and 1965, with a 0.2% random probability. This cluster is followed by a 36-yr gap (1965–2001) in earthquakes of $\mathbf{M} \geq 8.4$. Based on the Monte Carlo simulation, the probability of 18 random events during a period of 100 yr leaving a 36-yr gap is 0.5%. Thus the largest earthquakes in the 1900–2001 catalog show

Table 1
PScat2001 events of $M_0 \geq 20 \cdot 10^{20}$, ($\mathbf{M} \geq 8.167$), 1900–2001

Event No.	Date Year	Date mm/dd	hr/min	Latitude	Longitude	Depth, km	$M_0 \cdot 10^{20}$, N m	$\mathbf{M}$
1	1905	0709	0940	49.00	99.00	35	55	8.5
2	1905	0723	0246	49.00	97.00	35	50	8.4
3	1906	0131	1536	01.00	−81.30	33	80	8.6
4	1906	0817	0040	−33.00	−72.00	33	66	8.5
5	1917	0626	0549	−15.50	−173.00	33	70	8.5
6	1918	0815	1218	05.70	123.50	33	25	8.2
7	1918	0907	1716	45.50	151.50	33	22	8.2
8	1919	0430	0717	−19.00	−172.50	33	27.1	8.3
9	1920	1216	1205	36.60	105.40	33	30	8.3
10	1922	1111	0432	−28.50	−70.00	33	140	8.7
11	1923	0203	1601	54.00	161.00	33	70	8.5
12	1924	0626	0137	−55.00	158.40	33	30.2	8.3
13	1933	0302	1730	39.25	144.50	30	43	8.4
14	1938	0201	1904	−5.05	131.50	40	52	8.4
15	1943	0406	1607	−30.98	−71.27	20	25	8.2
16	1950	0815	1409	28.70	96.60	30	95	8.6
17	1952	1104	1658	52.75	159.50	33	350	9.0
18	1957	0309	1422	51.63	−175.41	33	100	8.6
19	1958	1106	2258	44.38	148.58	32	44	8.4
20	1960	0521	1002	−37.17	−72.96	33	20	8.2
21	1960	0522	1911	−38.20	−73.50	32	2000	9.5
22	1963	1013	0517	44.90	149.60	40	75	8.6
23	1964	0328	0336	61.10	−147.60	30	750	9.2
24	1965	0124	0011	−2.40	126.00	23	24	8.2
25	1965	0204	0501	51.30	178.60	35	140	8.7
26	1966	1017	2141	−10.92	−78.79	21	20	8.2
27	1968	0516	0048	40.90	143.40	35	28	8.3
28	1969	0811	2127	43.60	147.20	30	22	8.2
29	1977	0819	0608	−11.09	118.46	23	24	8.2
30	1979	1212	0759	01.60	−79.36	24	29	8.3
31	1989	0523	1054	−52.34	160.57	50	24	8.2
32	1994	1004	1323	43.60	147.63	68	30	8.3
33	1996	0217	0600	−0.67	136.62	15	24	8.2
34	2001	0623	2034	−17.28	−72.71	30	47	8.4

a distribution that is highly nonrandom, providing a statistical basis for the global moment release sequence discussed subsequently.

To further test the robustness of the clustering, the magnitudes of the earthquakes were perturbed to simulate random uncertainty in magnitude. We hypothesized that the observed magnitudes were the result of some original magnitude and some uncertainty in the determination of that magnitude. We assumed this uncertainty could reasonably be represented by a bounded, triangular distribution centered at zero and whose endpoints extended plus and minus 0.4 units.

What is needed is the distribution of possible original magnitudes, given an observed magnitude in a range 0.1 unit wide. This distribution cannot be symmetric, because in a Gutenberg–Richter distribution, there are more events in the magnitudes less than the range that can be "promoted" into the range by the assumed triangular distribution than events in the magnitudes greater than the range that can be "demoted" into the range.
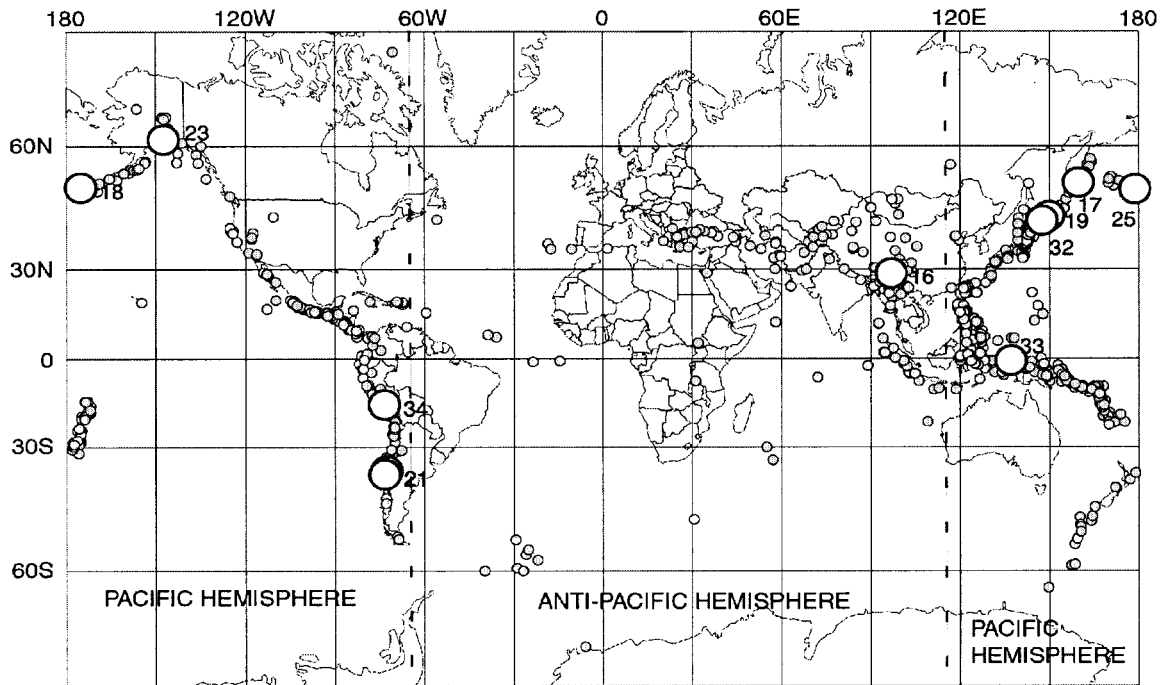
Figure 1.   Global distribution of **M** ≥ 7 earthquakes as a function of latitude and longitude from the Pacheco–Sykes catalog (1900–1989) extended in this article through 2001. The large, numbered circles are earthquakes referred to in the text. The corresponding numbers are refer to the **M** ≥ 8.2 earthquakes in Table 1. Boundaries between circum-Pacific hemisphere and anti-Pacific hemisphere are indicated by dashed lines.

The distribution of corrections to original magnitude was obtained by a Monte Carlo simulation, assuming a *b*-value of 1.5, that observed in the data set above magnitude 8.167 (corresponding to moment 20 × 10²⁰ N m, Table 1). Two hundred samples were required to get a sufficiently smooth distribution. This distribution would be expected to be bounded by a uniform distribution (−0.4, +0.4) and the original triangular distribution, but rather than symmetric, biased toward negative correction, as is indeed the case (Fig. 4).

With this correction distribution, 20 random synthetic catalogs were derived of "corrected" magnitudes at the observed dates, and the likelihoods of the observed clusters of **M** ≥ 8.95 and **M** ≥ 8.55 assessed in the same manner as in the original data (Fig. 5). In these catalogs, two or three events **M** ≥ 8.95 always occurred, and 19 of 20 times the significance level was less than 8%. (The 20th time the significance level was 15%.) Similarly, for events **M** ≥ 8.55, 16 of 20 times the significance level was less than 4%; 19 of 20 times the significance level was less than 13%. These results indicate the unlikelihood that the observed clustering can be attributed to magnitude uncertainty.

To test the likelihood of uncertainty in a different way, the observed dates were permuted among the observed magnitudes and the resulting groupings of the three **M** ≥ 8.95 assessed by the methods of this article. A group of 100 permutations was examined, and the results showed that 6 times of a 100, the significance level was smaller than 8%. This

permutation test gives a larger significance level than the previous test using corrected magnitudes, and would in itself suggest that the observed clustering of **M** ≥ 8.95 is less significant than calculated in this article, but still indicative of something unusual. However, clustering of **M** ≥ 8.55 accompanying the clustering **M** ≥ 8.95 is much more rare in the permuted catalogs. For each of the eight trials showing clustering of **M** ≥ 8.95, accompanying clustering of **M** ≥ 8.55 was not observed. This reinforces the unlikelihood that the observed historical period of high moment release is a statistical accident.

The significance of the post-1965 gap for **M** ≥ 8.35 was not tested for the magnitude-perturbed synthetic catalogs. However, at **M** ≥ 8.55, the 1965–2001 gap is evident in all 20 trials in Figure 5, and for 19 of 20 trials the gap continues to the end of the catalog. The Monte Carlo probability of chance occurrence of the continuing **M** ≥ 8.55 quiescence (39.8 yr) is 10%.

Global Moment Release

Individual earthquakes cited in this section are coded by number and further information can be found in Table 1. The event numbers shown in Figure 6–8 are also keyed to this table. Cumulative moment release for all earthquakes (**M** ≥ 7) in the catalog is shown in Figure 6a. Earthquakes in the circum-Pacific region dominate global moment release (Pacheco and Sykes, 1992). More than 92% of the global
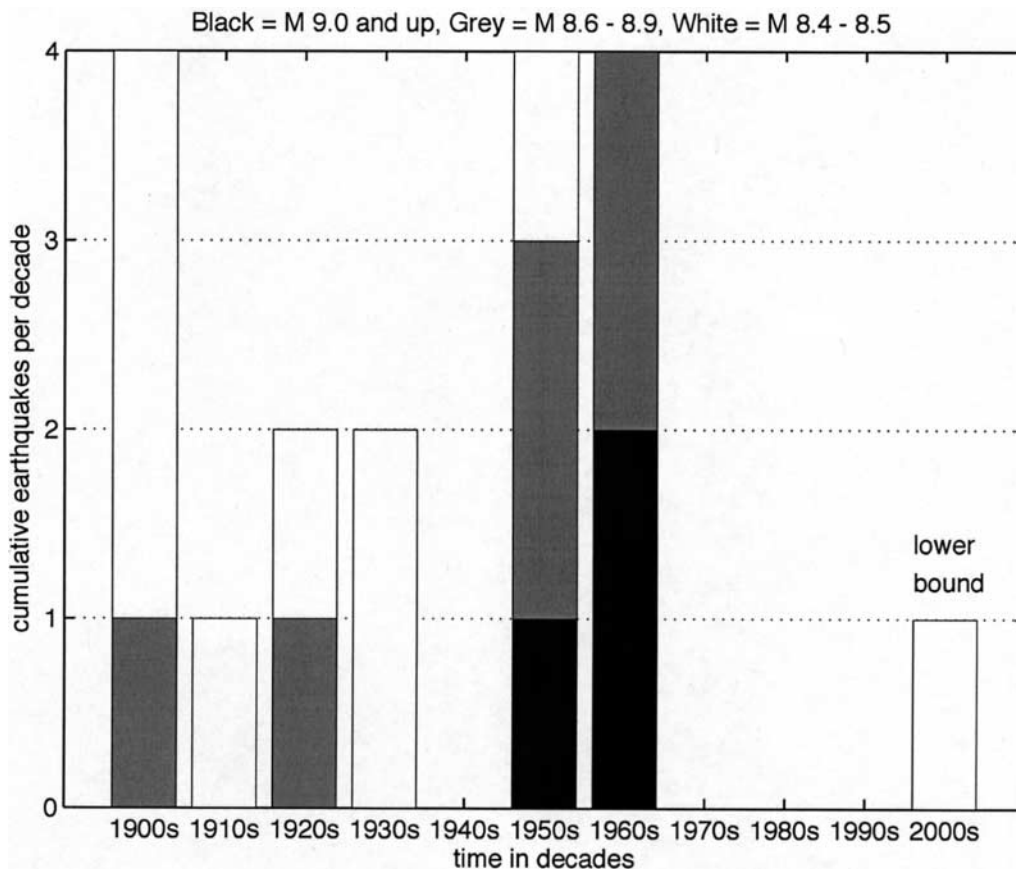
Black = M 9.0 and up, Grey = M 8.6 - 8.9, White = M 8.4 - 8.5

Figure 2.   Decadal histogram illustrating temporal clustering of global great earth-
quakes of **M** ≥ 9.0 (black), **M** ≥ 8.6 (black + gray), and **M** ≥ 8.4 (black + gray +
white). The bar for the 2000s is a lower bound, because only the first 2 yr of the decade
are represented.

moment release occurs in the Pacific hemisphere bounded
by longitudes 115° E and 65° W (see Fig. 1). When the less
than 8% of global moment release occurring in the other half
of Earth (the anti-Pacific hemisphere) is examined separately
(Fig. 6b), a pattern very similar to the global pattern
emerges, with a shift of about 10 yr. The dominant event,
the **M** 8.6 Assam earthquake, is the first in the 1950–1964
global cluster of great earthquakes cited before. It is the only
earthquake in the anti-Pacific hemisphere large enough to
make a significant contribution to the global–moment re-
lease sequence of Figure 7. The regional controlling role of
this earthquake was previously noted by Triep and Sykes
(1997).

The proposed global–moment release sequence is
shown in detail in Figure 7. The terms "global aftershock"
and "global foreshock" are used advisedly in this article,
with the understanding that the events so classified do not
meet the usual spatial and temporal criteria for more local-
ized sequences. The terminology is used to stress the simi-
larities and differences between the global sequence and typ-
ical sequences that occur along plate boundaries. Beginning
in mid-1924 (Fig. 7), worldwide seismic–moment release

rate was low. The rate increased sporadically over several
decades preceding the great **M** 9.5 Chile earthquake of May
1960 (global mainshock, event 21), most dramatically in the
1950s. Decadal–moment release rates accelerated (Fig. 7)
from $3 \cdot 10^{21}$ N m/yr in 1930–1940 to $8 \cdot 10^{21}$ N m/yr in 1950–
1960, with a hiatus in the 1940s. Principal global foreshocks
to the 1960 event were the **M** 8.6 Assam earthquake (event
16) of August 1950, the **M** 9.0 Kamchatka earthquake (event
17) of November 1952, the **M** 8.6 central Aleutian earth-
quake (event 18) of March 1957, and the **M** 8.4 south Kuril
Islands earthquake (event 19) of November 1958. Immedi-
ately after the **M** 9.5 Chile earthquake, the moment release
rate was very low ($7 \cdot 10^{20}$ N m/yr) for 3.4 yr until the oc-
currence of the **M** 8.5 south Kuril Islands earthquake (event
22) in October 1963. Major moment release continued with
the occurrence of the **M** 9.2 Alaskan earthquake (event 23)
of March 1964, and the **M** 8.7 Rat Islands earthquake (event
25) of February 1965. The global moment rate then system-
atically decelerated from a decadal average of $1.2 \cdot 10^{22}$ N m/
yr from mid-1960 through 1969 to a low of $1.5 \cdot 10^{21}$ N m/
yr in 1980 through 1989. With the advent of routine moment
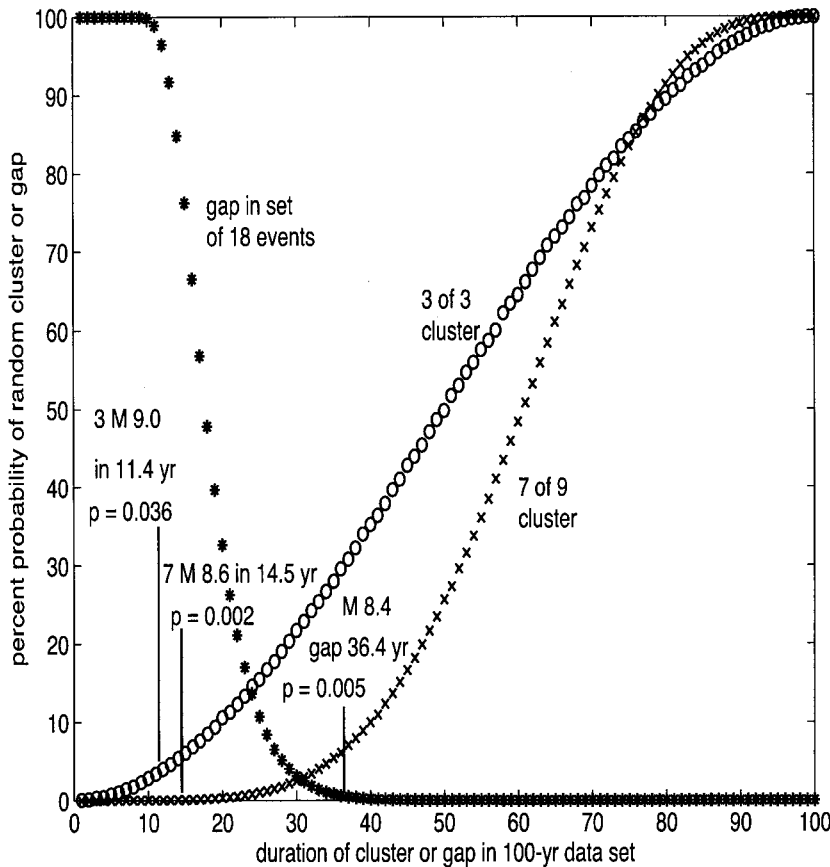tensor computation in the late 1970s, the apparent noise level

Figure 3. Probabilities of random occurrence of the observed global earthquake clusters and gaps. Each probability curve is derived by using a Monte Carlo approach with 100,000 simulations. Probabilities are low that the observed clustering and quiescence would be observed in a random series of earthquakes.

in the data is reduced, and sharply defined temporal patterns in the global–moment release data can be seen. A low ambient or background global–moment release rate of about $1 \cdot 10^{21}$ N m/yr is punctuated by the occurrence of larger events ($M_0 \geq 2 \cdot 10^{21}$), some of them preceded by periods of accelerating moment release. The pattern of continuing deceleration appears to have clearly ended with the occurrence of the Off-Iturup (south Kuril Islands) earthquake (event 32) of October 1994. At **M** 8.3, this event was arguably the largest earthquake since the 1965 Rat Islands earthquake. The **M** 8.4 earthquake (event 34) of June 2001 off southern Peru was the largest to occur in more than 36 years. The average moment rate (October 1994 through December 2001) has increased to $4 \cdot 10^{21}$ N m/yr, the highest sustained rate since the 1960s and comparable with the 1930s. The increase in moment rate beginning in 1994 is also evident in the annual moment summaries of Dziewonski *et al.* (1999). A sharper increase in moment rate is apparent in the anti-Pacific hemisphere (Fig. 6b), from $1 \cdot 10^{20}$ N m/yr in 1990–1999 to $12 \cdot 10^{20}$ N m/yr during 2000–2001.

A Global Seismic Cycle?

The observed global–moment release pattern (large-event clustering, with acceleration before and deceleration after the mainshock) is similar to behavior observed on a regional scale in the greater San Francisco Bay region (see,

for instance, Sykes and Jaume [1990]; Bufe and Varnes [1993]). This suggests that Earth, over many decades, may also respond as a coherent, nonrandom, nonlinear system of stress redistribution. If there is a global seismic cycle and it is approximated by the observed (1924–1994) sequence, the duration is about 70 ± 10 yr, with the greater earthquakes (**M** $\geq$ 8.6) clustered within a period of 15 yr. By analogy to the seismic cycle of the greater San Francisco Bay region (Bufe and Varnes, 1993), there may be self-similar subcycles or episodes on different magnitude and time scales within the global seismic cycle. The observed global sequence has a time scale similar to that of the subcycle leading to the occurrence of the 1989 **M** 7 Loma Prieta, California, earthquake. It is unlikely that the observed sequence is such a subcycle, because this would imply the occurrence of earthquakes (or possibly swarms) with seismic moment much greater than that of the 1960 Chile earthquake.

If the concept of a global seismic cycle is valid, and if this is the phenomenon we have observed, then the global-cycle durations will be shorter than the recurrence times of most individual great earthquakes, because not all the global potential seismic moment or energy is released in a single cycle.

With regard to a different category of global subcycles, our proposed global seismic cycle contains the three 20- to 30-yr global cycles of alternating toroidal (strike slip) and poloidal (thrust or normal) energy release noted by Roma-
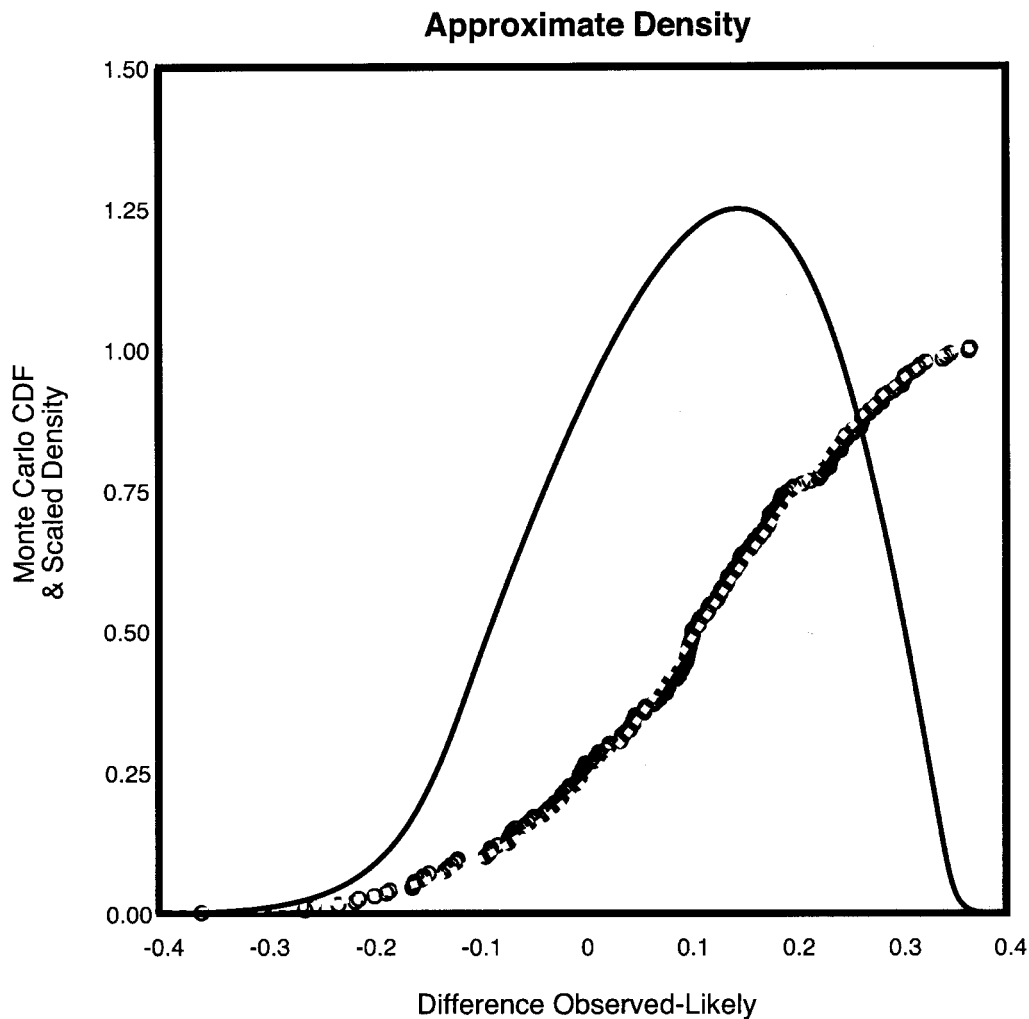
Approximate Density

Figure 4. Distribution of observed minus likely original magnitude, obtained by a Monte Carlo simulation, assuming a *b*-value of 1.5, and an uncertainty distribution for measurement error assumed to be triangular (-0.4, $+0.4$) Two hundred samples were required to get a sufficiently smooth distribution. The negative of this distribution is used to get alternative catalogs of original magnitude in Monte Carlo simulations.

nowicz (1993). The central, poloidal cycle corresponds to the period of high moment release in the 1950s and 1960s and is flanked by lower-moment toroidal cycles, most notably during the gap for $\mathbf{M} \geq 8.4$ that extends from 1965 to 2001. Global seismic cycles are likely to be even more complex than those involving a specific segment of a plate boundary, in that both the duration of the cycle, and the locations of the suite of temporally clustered, great thrust earthquakes responsible for the surge of moment release, may vary from cycle to cycle.

Varnes (1989) and Bufe and Varnes (1993) have studied the power-law dependence of accelerating seismic-moment and Benioff strain release as a tool for earthquake forecasting based on a time-to-failure model. The model is governed by the equation:

$$\Sigma\Omega = K + (k/(n - 1))(t_f - t)^m \qquad (2)$$

where Ω is a measure of seismic release calculated from magnitude, K, k, and n are constants, $m = 1 - n$ ($n < 1$), and t_f is time of failure (mainshock). Using this model, Bufe *et al.* (1994) made a successful forecast (3-yr window) of the June 1996 $\mathbf{M}$ 7.9 earthquake on the Delarof segment of the Aleutian arc, the largest earthquake to be recorded on this segment. If the model can be extended to a global scale, it may be possible to forecast the greatest earthquakes within a decade or so, although there may not be a way of determining where on Earth the earthquake would occur. With the magnitude and occurrence time constrained, the accelerating global moment release for 22 earthquakes of $\mathbf{M} \geq 8$ over a 30-yr period preceding the 1960 Chile earthquake can be described (Fig. 8) as a power-law dependence on remaining time to failure with an exponent of 0.1.

The gradual decay in moment rate after the 1960 Chile earthquake and continuing until 1994 may be analogous to
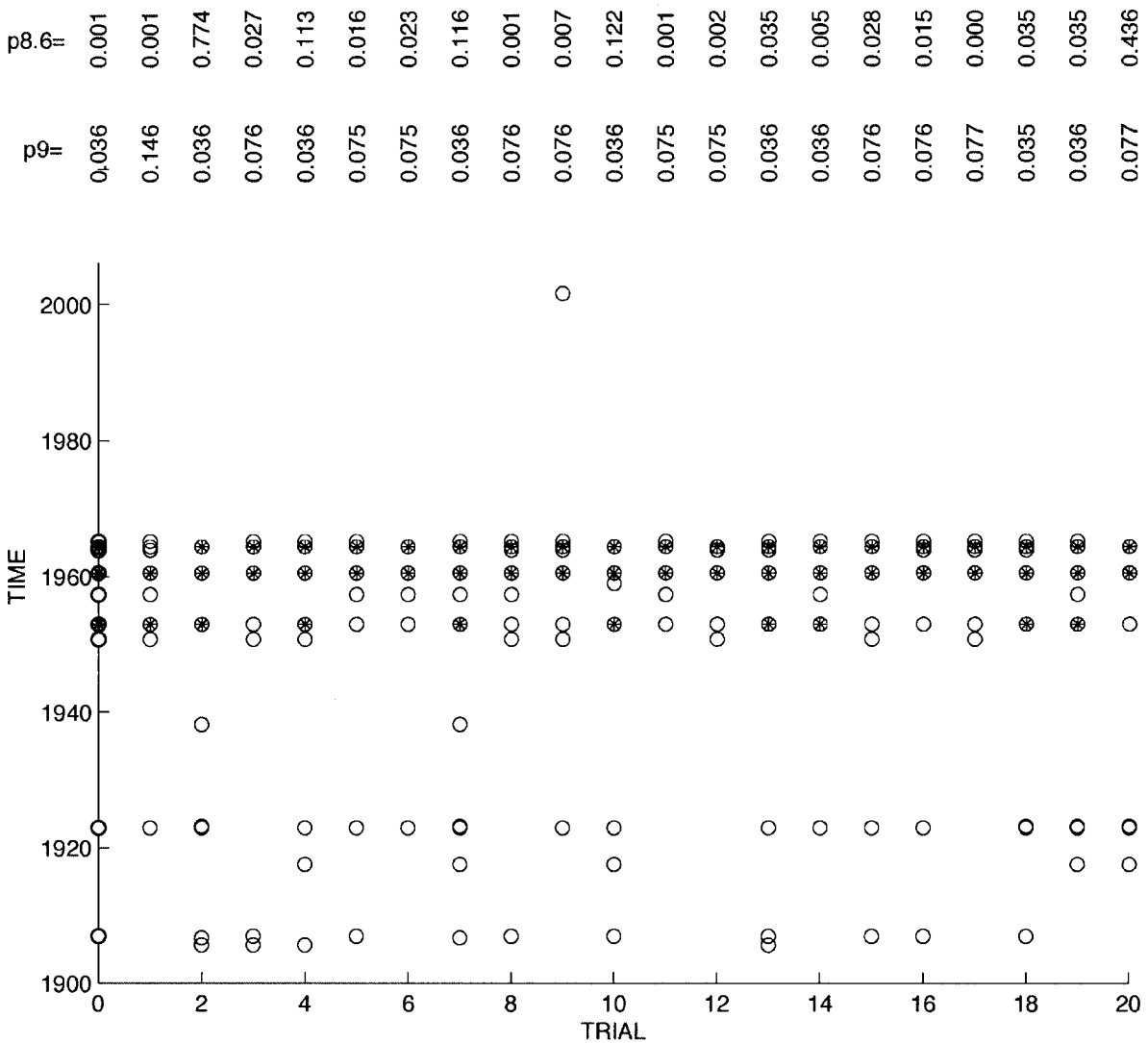
Figure 5. Twenty random synthetic catalogs were derived of "corrected" magnitudes at the observed dates by using the magnitude-difference distribution of Figure 4. Likelihoods of the observed clusters of **M** ≥ 8.95 (filled circles) and **M** ≥ 8.55 (open circles) were assessed in the same manner as in the original data, which are plotted as trial zero. For some closely clustered events, the open circles may overlap or effectively coincide.

an aftershock sequence fading into a stress shadow on a global scale. This trend was terminated by the recent increase in global moment rate, the highest rate since the 1960s and comparable with the 1930s. This increase in global–moment release rate in both the Pacific and anti-Pacific hemispheres may be related to the recent change in moment of inertia and shape of the earth (Cox and Chao, 2002). Dickey *et al.* (2002) attribute the observed increase in oblateness to subpolar glacial melting and mass shifts in the oceans.

Global Triggering

The existence of large-scale temporal earthquake clustering and quiescence is not surprising given the statistical results of Kagan and Jackson (1991) indicating significant long-term and long-range correlations. Keilis-Borok and colleagues (for example, Keilis-Borok and Rotwain, [1990]) developed the **M** 8 earthquake prediction algorithms based on statistical analysis of earthquake occurrence patterns in very large regions. The radius of the **M** 8 zone of earthquake preparation or "flow activation" scales with the magnitude of the target earthquake, such that:

$$D = \exp(M - 5.6) + 1 \qquad (3)$$

where D is the epicentral distance in degrees. Using this scaling relation with the moment magnitudes cited previously, the radius of the zone of preparation of the 1960 Chile earthquake approaches or exceeds the radius of the earth.
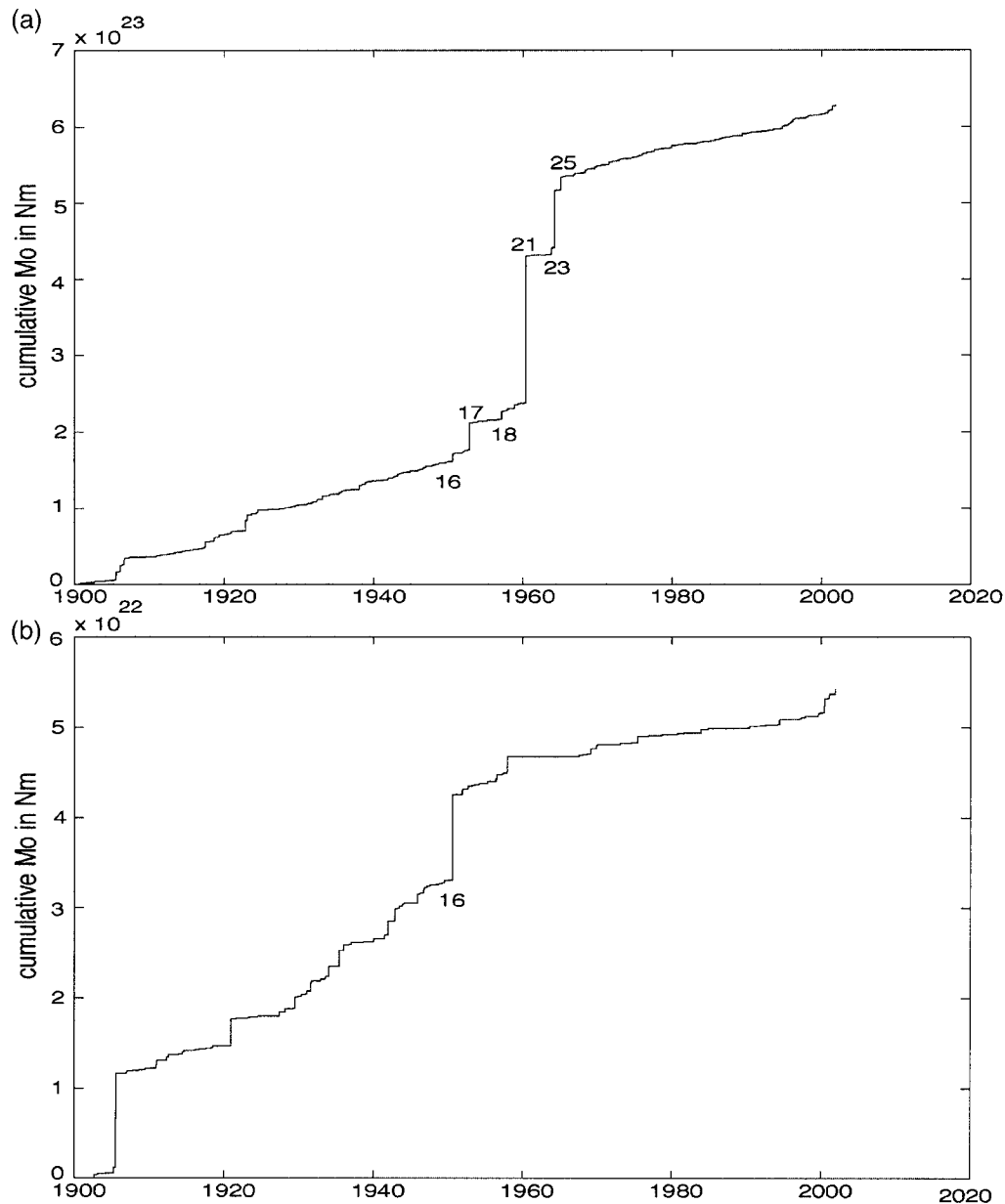
Figure 6. Cumulative moment release, 1900–2001, for **M** ≥ 7 earthquakes. (a) Global-moment release. (b) Moment release in the anti-Pacific hemisphere, 65° W to 115° E.

To explain the global clustering and quiescence demonstrated in Figures 2 and 3, a very-large-scale mechanism for global earthquake triggering and/or stress transfer is required. There are several candidates, but none has been convincingly demonstrated on a global scale. A characteristic of the mechanism (or mechanisms) is a long time constant or relatively slow propagation rate, indicated by the lack of short-term clustering of distant great earthquakes. For example, an anomalously low global–moment release rate followed the great 1960 Chile earthquake for more than 3 yr.

Investigation of mechanisms for global triggering is beyond the scope of this article, but there are many possibilities, among them:

1. Quasi-static changes in fault properties or pore pressure induced by transient dynamic stresses of seismic waves or free oscillations of the earth generated by distant great earthquakes.
2. Propagation of viscoelastic deformation in the aesthenosphere (Piersanti *et al.*, 1995; Pollitz *et al.*, 1998).
3. Stress transfer from great slow earthquakes (such as the precursor to the great 1960 Chile earthquake) migrating along the base of the seismogenic zone along plate margins.
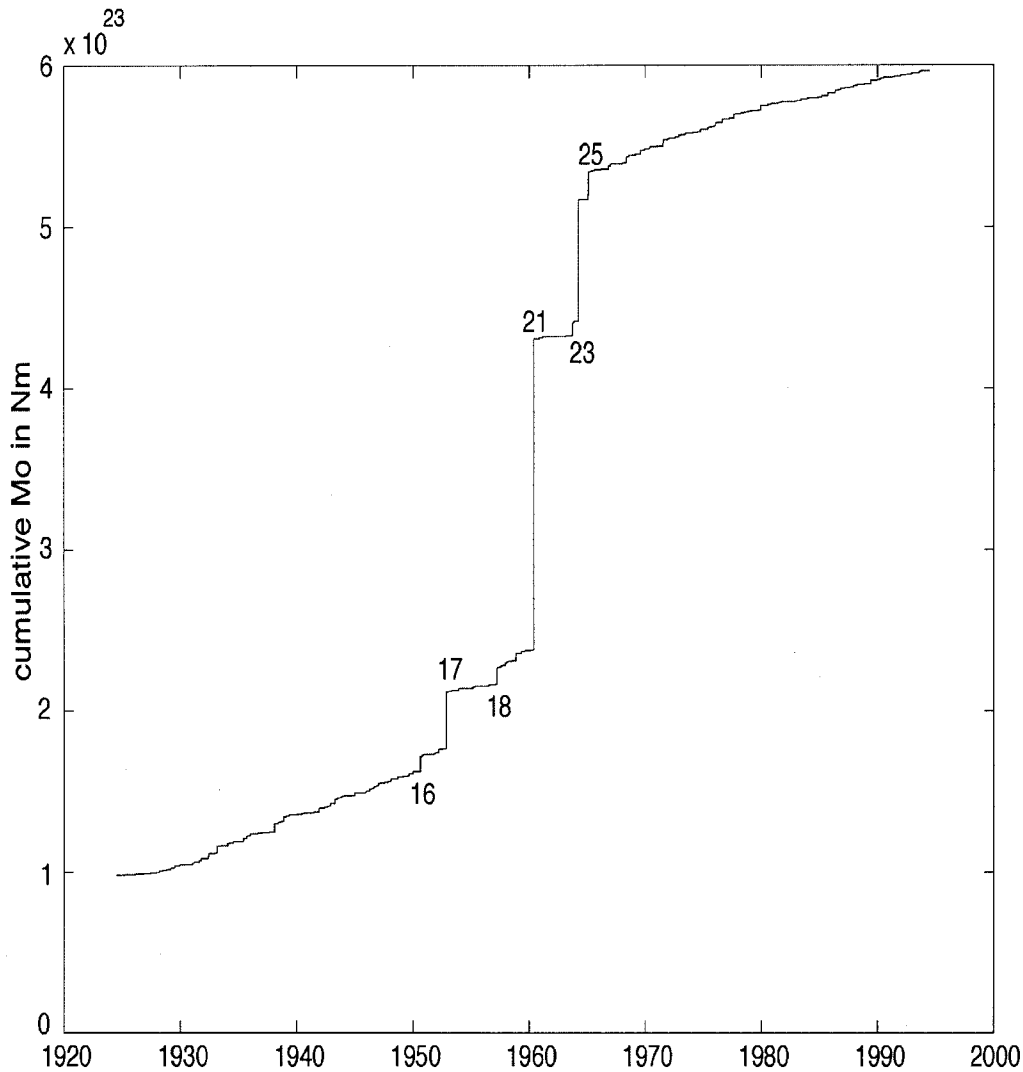4. Earth's adjustment to global redistribution of mass in the hydrosphere or mantle.

Figure 7. Global-moment release sequence, 1924–1994, for **M** ≥7 earthquakes.

5. Attainment of a global tectonic state of self-organized criticality.

Global modeling of postearthquake viscoelastic deformation by Piersanti *et al.* (1995) has demonstrated its potential for earthquake triggering, and viscoelastic triggering effects of the great 1952–1965 subduction earthquakes in the north Pacific region were documented by Pollitz *et al.* (1998) to distances of 4000 km over four decades.

Conclusions

Based on data from an extended Pacheco–Sykes catalog, temporal clustering in a 12-yr period (1952–1964) of the three greatest (**M** ≥ 9.0) earthquakes and in a 15-yr period (1950–1965) of seven of the nine greatest earthquakes to occur in the past century is highly significant. Monte Carlo simulations of random occurrence suggest that the probabilities of such clustering occurring randomly are 4% and 0.2%, respectively. The observed 36-yr quiescence at **M** ≥ 8.4 (global stress shadow) after the 15-yr cluster is also highly significant, with a 0.5% probability of random occurrence. In alternative catalogs derived by correcting for probable random errors in the extended Pacheco–Sykes catalog, the clustering at **M** ≥ 9 persists at a significance level of less than 8%. When the catalog magnitudes and times are randomly shuffled, Monte Carlo simulations indicate that significant clustering of the three **M** ≥ 9 events occurs in 6 of 100 trials. However, unlike the actual catalog, none of the trials show significant clustering at **M** ≥ 8.6. This suggests that the probability of random occurrence of the observed concurrent clustering of both **M** ≥ 9 and **M** ≥ 8.6 earthquakes is 1% or less.

Cumulative moment release data provide evidence of a 70 ± 10-yr global sequence or seismic cycle, consisting of a period of accelerating moment release (global foreshocks), a mainshock (the 1960 **M** 9.5 Chile earthquake), and a 30-yr period of decelerating moment release (global after-
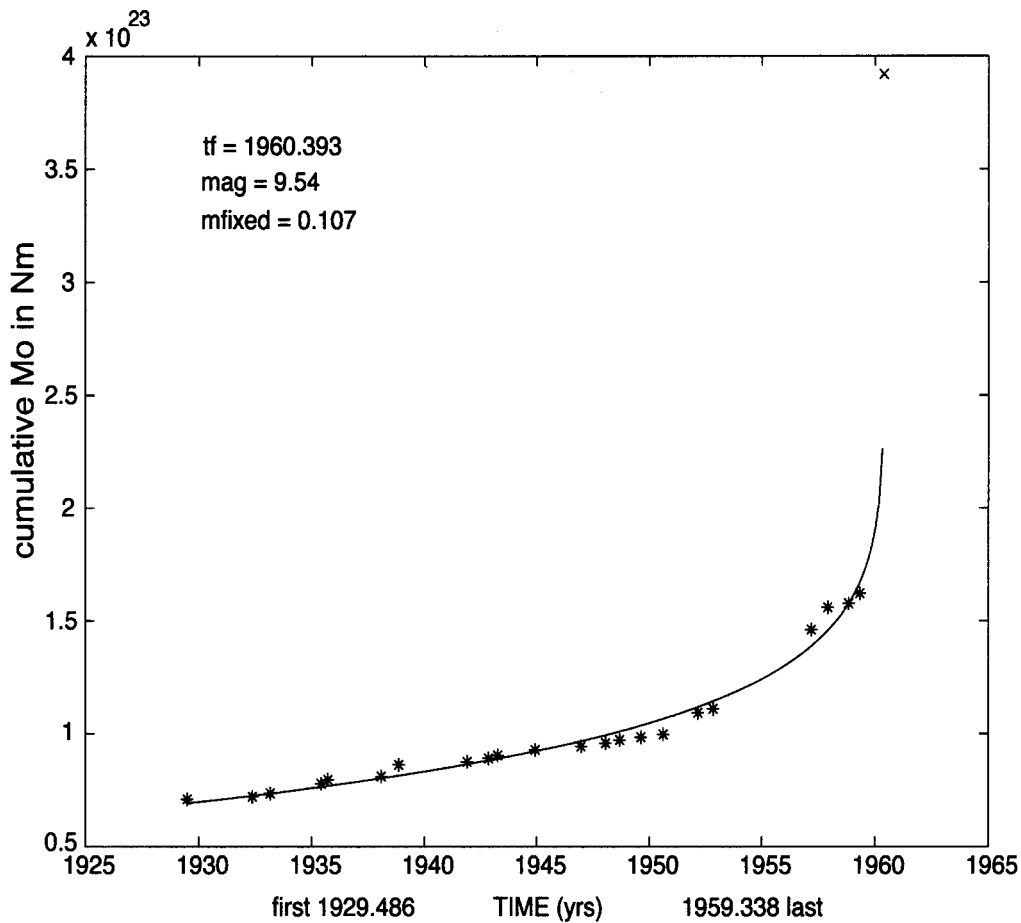
Figure 8. Power-law dependence on the remaining time to failure of global accelerating moment release of **M** ≥8 events preceding the great 1960 Chile earthquake. The theoretical curve is generated using equation (1) with time of failure, t_f, constrained.

shocks). During the sequence, seven earthquakes of **M** ≥ 8.6 occur. These include the **M** 9.5 global mainshock, three great global foreshocks (**M** 8.6, 9.0, and 8.6) in the preceding 10 yr, and three great global aftershocks (**M** 8.6, 9.2, and 8.7) in the following 5 yr. Global moment rates continued to decrease until the early 1990s. From late 1994 through 2001, the rate appears to be increasing and is comparable with that of the 1930s. On close examination, abrupt short-term changes in the global–moment release rate are observed from 1990 through 2001, punctuated by the occurrence of **M** ≥ 8.2 earthquakes. The largest event during this period was the **M** 8.4 southern Peru earthquake of June 2001. This was the largest earthquake since the **M** 8.7 earthquake of February 1965. The increased rate of moment release in 1994–2001 is the highest sustained rate observed since 1965 and may mark the beginning of the acceleration phase of a new global cycle. Increases in moment rate were also observed in the anti-Pacific hemisphere preceding the great 1960 Chile earthquake and again during 2000–2001. All of the preceding suggests that global moment release is not random and that the processes involved may be globally coherent on a time scale of a decade or so.

Note Added to Proof

In the present article, we discussed the subsequent surge in moment release from 2000 to 2001 in both the Pacific and anti-Pacific hemispheres and the significance of occurrence in June 2001 of the **M** 8.4 Peru event, and we suggested that a new global cycle may have begun. On 26 December 2004, a mega-quake (our term for an earthquake of **M** ≥9) occurred off the coast of Sumatra. The recent occurrences of this mega-quake and the adjacent (to the southeast) rupture of a **M** 8.7 Sumatra event of 28 March 2005, confirm that we have entered a new period of high moment release and probable temporal clustering of mega-quakes.

Was there similar clustering in the 1800s? Abe (1979) noted the clustered occurrence of pairs of M_t 9 (tsunami magnitude) earthquakes from 1837–1841 and from 1868–1877. An earlier probable mega-quake occurred southeast of the 2005 Sumatra event in 1833 (Zachariasen *et al.*, 1999), extending Abe's first cluster to 1833–1841. To the extent the Abe catalog is complete for mega-quakes during the earlier period, we can draw some additional conclusions on the basis of this clustering. The duration of the mega-quake phase

of the global cycles has been 8, 9, and 12 years, with intervening periods of 27, 75, and 52 years. (As we indicated earlier, the timing and duration of global seismic cycles would not be expected to be uniform.) Hence, we would anticipate the period of additional mega-quakes following the 2004 Sumatra event would last about a decade.

Acknowledgments

References

Abe, K. (1979). Size of great earthquakes from 1837–1974 inferred from tsunami data, *J. Geophys. Res.* **84,** 1561–1568.

Barrientos, S. E., and S. N. Ward (1991). The 1960 Chile earthquake: inversion for slip distribution from surface deformation, *Geophys. J. Int.* **103,** 589–598.

Benioff, V. H. (1951). Global strain accumulation and release as revealed by great earthquakes, *Bull. Geol. Soc. Am.* **62,** 331–338.

Benioff, V. H. (1954). Evidence for world-strain readjustment following the Kamchatka earthquake of 4 November 1952, *Bull. Geol. Soc. Am.* **65,** 1332–1333.

Bufe, C. G. (1997). 1924–1994: evidence for a global moment release sequence, *EOS Trans. AGU* **78,** F476.

Bufe, C. G., and D. J. Varnes (1993). Predictive modeling of the seismic cycle of the greater San Francisco Bay region, *J. Geophys. Res.* **98,** 9871–9883.

Bufe, C. G., S. P. Nishenko, and D. J. Varnes (1994). Seismicity trends and the potential for large earthquakes in the Alaska-Aleutian region, *Pure Appl. Geophys.* **142,** Special Issue on Shallow Subduction Zones, 83–99.

Cifuentes, I. (1989). The 1960 Chilean earthquakes, *J. Geophys. Res.* **94,** 665–680.

Cifuentes, I., and P. Silver (1989). Low-frequency source characteristics of the Great 1960 Chilean earthquake, *J. Geophys. Res.* **94,** 643–663.

Cox, C., and B. F. Chao (2002). Detection of large-scale mass redistribution in the terrestrial system since 1998, *Science* **297,** 831–833.

Davies, G., and J. Brune (1971). Regional and global fault slip rates from seismicity, *Nature Phys. Sci.* **229,** 101–107.

Dickey, J. O., S. L. Marcus, O. de Viron, and I. Fukumori (2002). Recent earth oblateness variations: unraveling climate and postglacial rebound effects, *Science* **298,** 1975–1977.

Dziewonski, A. M., G. Ekstrom, and N. N. Maternovskaya (1999). Centroid-moment tensor solutions for October-December 1998, *Phys. Earth Planet. Interiors* **115,** 1–16.

Dziewonski, A. M., G. Ekstrom, and N. N. Maternovskaya (2001). Centroid-moment tensor solutions for April-June 2000, *Phys. Earth Planet. Interiors* **123,** 1–14.

Hanks, T. C., and H. Kanamori (1979). A moment magnitude scale, *J. Geophys. Res.* **84,** 2348–2350.

Kagan, Y. Y., and D. D. Jackson (1991). Long-term earthquake clustering, *Geophys. J. Int.* **104,** 117–133.

Kanamori, H., and D. L. Anderson (1975a). Theoretical basis of some empirical relations in seismology, *Bull. Seism. Soc. Am.* **65,** 1073–1095.

Kanamori, H., and D. L. Anderson (1975b). Amplitude of the earth's free oscillations and long-period characteristics of the earthquake source, *J. Geophys. Res.* **80,** 1075–1078.

Kanamori, H., and J. Cipar (1974). Focal process of the great Chilean earthquake May 22, 1960, *Phys. Earth Planet. Interiors* **9,** 128–136.

Keilis-Borok, V. I., and I. M. Rotwain (1990). Diagnosis of time of increased probability of strong earthquake in 12 regions of the world, *Phys. Earth Planet. Interiors* **61,** 57–72.

Mogi, K. (1974). Active periods in the world's chief seismic belts, *Tectonophysics* **22,** 265–282.

Mogi, K. (1979). Global variation of seismic activity, *Tectonophysics* **57,** T43–T50.

Pacheco, J. F., and L. R. Sykes (1992). Seismic moment catalog of large shallow earthquakes, 1900 to 1989, *Bull. Seism. Soc. Am.* **82,** 1306–1349.

Piersanti, A., G. Spada, R. Sabadini, and M. Bonafede (1995). Global postseismic deformation, *Geophys. J. Int.* **120,** 544–566.

Plafker, G., and J. C. Savage (1970). Mechanism of the Chilean earthquakes of May 21 and 22, 1960, *Bull. Geol. Soc. Am.* **81,** 1001–1030.

Pollitz, F. F., R. Burgmann, and B. Romanowicz (1998). Viscosity of oceanic asthenosphere inferred from remote triggering of earthquakes, *Science* **280,** 1245–1249.

Romanowicz, B. (1993). Spatiotemporal patterns in the energy release of great earthquakes, *Science* **260,** 1923–1926.

Sykes, L. R., and S. C. Jaume (1990). Seismic activity on neighboring faults as a long-term precursor to large earthquakes in the San Francisco Bay area, *Nature* **348,** 595–599.

Triep, E. G., and L. R. Sykes (1997). Frequency of occurrence of moderate to great earthquakes in intracontinental regions: Implications for changes in stress, earthquake prediction, and hazards assessment, *J. Geophys. Res.* **102,** 9923–9948.

Varnes, D. J. (1989). Predicting earthquakes by analyzing accelerating precursory seismic activity, *Pure Appl. Geophys.* **130,** 661–686.

Zachariasen, J., K. Sieh, F. W. Taylor, and W. S. Hantoro (1999). Submergence and uplift associated with the giant 1833 Sumatran subduction earthquake: evidence from coral microatolls, *J. Geophys. Res.* **104,** 895–919.

U.S. Geological Survey
Central Region Geologic Hazards Team
P.O. Box 25046, MS966
Denver, Colorado 80225
cbufe@usgs.gov
perkins@usgs.gov